J. Cent. South Univ. (2014) 21: 3787−3792
DOI: 10.1007/s11771-014-2363-z

Springer

Characteristics of unsteady lubrication film in metal-forming process with dynamic roll gap

WANG Qiao-yi(王桥医)[1], ZHANG Ze(张泽)[1], CHEN Hui-qin(陈慧勤)[1], GUO Shan(过山)[1], ZHAO Jing-wei(赵敬伟)[2]

1. School of Mechanical Engineering, Hangzhou Dianzi University, Hangzhou 310018, China;
2. School of Mechanical, Materials and Mechatronic Engineering, University of Wollongong, NSW 2522, Australia

Abstract: Based on the theory of unsteady hydrodynamic lubrication and relevant mathematic and physical methods, a basic model was developed to analyze the unsteady lubrication film thickness, pressure stress and friction stress in the work zone in strip rolling. The distribution of pressure stress and friction stress in the work zone was obtained. A numerical simulation was made on a 1850 cold rolling mill. The influence of back tension stress and reduction on the distribution of pressure stress and friction stress between the roll gaps was qualitatively analyzed by numerical simulation. The calculated results indicate that the higher the back tension, the lower the pressure stress and the friction stress in the work zone, and the largest friction stresses are obtained at the inlet and outlet edges. The pressure and friction gradients are rather small at high back tension. The pressure-sensitive lubricant viscosity increases exponentially with the increase of pressure. The unsteady lubrication phenomenon in the roll bite is successfully demonstrated.

Key words: metal-forming; interface; unsteady lubrication; dynamical roll gap; film characteristics

1 Introduction

The lubrication system is in a steady state in many metal forming processes, and the unsteady item in the Reynolds equation can be omitted. For the metal forming process with unsteady lubrication system or the structure in a vibration state [1−4], the unsteady items can not be omitted, and a complicated forming process will be encountered in this case since the process parameters are related to time. The lubrication state is no longer steady due to the appearance of vibration. In rolling process, unsteady lubrication caused by flutter belongs to this kind. Therefore, rolling process is a transient process that is related to time [5−6]. Due to the vibration of the machine structure, the lubrication system is in an unsteady state [7−9], and the friction is also related to time. In metal forming process, significant production losses involve the unsteady situation. Because rolling is one of the most important large deformation metal forming [10−12] processes, an in-depth understanding of unsteady lubrication phenomenon is therefore of great significance to build a more realistic friction model [13−15] in unsteady process, and a more accurate mechanical model of rolling process can be established. However, the existing friction model of rolling process is usually considered to be in a steady state. Based on the theory of unsteady hydrodynamic lubrication and relevant mathematic and physical methods, it is of importance to establish a basic model of unsteady lubrication for the film thickness, pressure stress and friction stress in the work zone in strip rolling, and then the distribution information of pressure stress and friction stress in the work zone is obtained.

2 Dynamic roll gap model

The geometry of the roll gap is shown in Fig. 1. In this figure, u is the strip speed change along the direction of horizontal x, v is the roll speed, x_1 is the length of the steady state in work zone, y_1 is the inlet strip thickness, y_2 is the outlet strip thickness, u_1 is the inlet strip speed, and u_2 is the outlet strip speed. Considering vertical vibration of the rolling, YUN et al [16] proposed a continuity equation of the roll bite as follows:

$$uy = u_1 y_1 - (x_1 - x)\dot{y}_c \tag{1}$$

where $\dot{y}_c$ is the change rate of roll gap spacing along the centerline of the rolls. The change of the roll gap is caused by the movement of the rolling structure. Before the rolling vibration model is determined, the change of the roll gap will not be considered. Therefore, the strip

Foundation item: Project(51175133) supported by the National Natural Science Foundation of China
Received date: 2013−05−29; **Accepted date:** 2013−10−23
Corresponding author: WANG Qiao-yi, Professor, PhD; Tel: +86−731−86878582; E-mail: wangqiaoyi1989@163.com

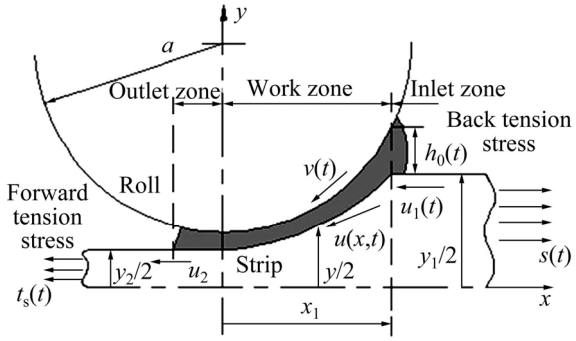

Fig. 1 Geometry of roll bite

speed in the work zone can be identified as

$$u = u_1 \frac{y_1}{y} = u_2 \frac{y_2}{y} \tag{2}$$

where y is the trip thickness in the work zone which can be identified as [17]

$$y = y_1(1-R) + \frac{x^2}{a} \tag{3}$$

where a is the roll radius, and R is the reduction which can be expressed as

$$R = \frac{y_1 - y_2}{y_1} \tag{4}$$

So the mean surface speed in the work zone u_m can be solved by Eqs. (2) and (3):

$$u_{1,m} = \frac{u+v}{2} = u_{1,m} + \frac{u_1}{2}\left[\frac{ay_1R - x^2}{ay_1(1-R)+x^2}\right] \tag{5}$$

where $u_{1,m}=(u_1+v)/2$. Because the gradient of roll bite pressure is much smaller than that of the inlet pressure, the pressure gradient in the Reynolds equation can be ignored. Therefore, Reynolds equation can be rewritten as

$$\frac{\partial u_m}{\partial x} + u_m \frac{\partial h}{\partial x} - \frac{\partial h}{\partial t} = 0 \tag{6}$$

where h is the film thickness in the work zone, and u is the mean surface speed. Equation (6) is a first-order partial differential equation, which can be broken down into two general differential equations as

$$\frac{\mathrm{d}x}{\mathrm{d}t} = -u_m \tag{7}$$

$$\frac{\mathrm{d}h}{\mathrm{d}x} = -\frac{h}{u_m}\frac{\partial u_m}{\partial x} \tag{8}$$

The two general differential equations above can be solved by using a mathematical method. The distribution of oil film thickness in the work zone is described in Eq. (8), and the physical meaning of u_m is the speed of emulsion flowing along the rolling direction. The change of oil film thickness depends on the speed of emulsion flowing along the rolling direction. This relationship also indicates that the thickness of oil film will decrease with the increase of the speed of emulsion flowing along the x direction. It can be seen that the thickness of oil film will reach the minimum on the edge of outlet in the work zone. Therefore, the outlet zone will be the critical point of the strip surface with good or bad quality.

3 Nondimensional interface variables

The nondimensional variables in the work zone are

$$\tilde{x} = \frac{x}{x_{10}} \tag{9}$$

$$H = \frac{h}{h_{00}} \tag{10}$$

$$U = \frac{u_m}{v_0} \tag{11}$$

where x_{10} is the length in the steady work zone, h_{00} is the film thickness in the steady inlet zone, and v_0 is the rolling speed in the steady state.

The nondimensional time scale in the work zone is based on the time of the roll surface passing through the work zone. The nondimensional time in the work zone is defined as

$$T = \frac{t}{x_{10}/v_0} = \frac{tv_0}{x_{10}} \tag{12}$$

Because the strip moves at different speed in the work zone, the strip through the actual time in the work zone is not equal to x_{10}/v_0.

Using the above defined nondimensional variables, Eqs. (7) and (8) can be rewritten as

$$\frac{\mathrm{d}\tilde{x}}{dT} = -U \tag{13}$$

$$\frac{\mathrm{d}H}{d\tilde{x}} = -\frac{H}{U}\frac{\partial U}{\partial \tilde{x}} \tag{14}$$

Both sides of Eq. (5) are divided by v_0, and then x is dimensionless:

$$U = U_{1,m} + \frac{U_1}{2}\left[\frac{1}{1+R(\tilde{x}^2-1)} - 1\right] \tag{15}$$

Equation (15) about x is derivative as

$$\frac{\partial U}{\partial \tilde{x}} = -\frac{U_1 R\tilde{x}}{[1+R(\tilde{x}^2-1)]^2} \tag{16}$$

When T=0, the initial conditions of the coupling Eqs. (13) and (14) are

$$T = 0, \tilde{x} = 1, H = 1 \tag{17}$$

At an arbitrary time T, the initial conditions of the coupling Eqs. (13) and (14) are

$$\tilde{x} = \tilde{x}_1, H = H_0 \tag{18}$$

where $\tilde{x}_1 = x_1/x_{10}$, $H_0 = h_0/h_{00}$, and h_0 is the film thickness between the work area and inlet area.

Numerical solving process can be carried out by a mathematical software Mathematica.

4 Determination of distribution of oil film friction stress and pressure stress

WILSON and CHANG [18] solved the pressure distribution in steady work zone. The steady lubrication analysis will use the calculated pressure and friction stress of every time step in the current unsteady situation instead.

Figure 2 shows a micro-unit body of the strip. The force balance equation in the x-direction is

$$-sy + (s + \mathrm{d}s)(y + \mathrm{d}y) + 2p(\frac{1}{2}\frac{\mathrm{d}y}{\mathrm{d}x})\mathrm{d}x + 2\tau_{\mathrm{f}}\mathrm{d}x = 0 \tag{19}$$

where s is the strip tension stress, y is the strip thickness in work zone, p is the local pressure stress, and τ_{f} is the local friction stress. Ignoring the relatively small items of Eq. (19), it is obtained

$$s\frac{\mathrm{d}y}{\mathrm{d}x} + y\frac{\mathrm{d}s}{\mathrm{d}x} + p\frac{\mathrm{d}y}{\mathrm{d}x} + 2\tau_{\mathrm{f}} = 0 \tag{20}$$

Based on the plastic flow rule [19] at any position in the work zone, there is

$$s + p = \sigma \tag{21}$$

where σ is the material yield stress. It follows

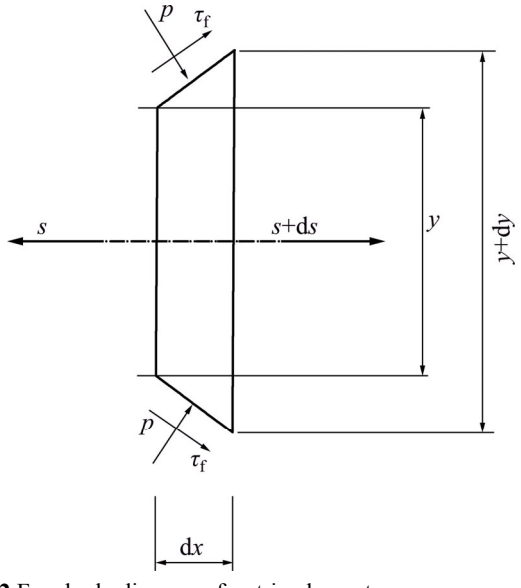

Fig. 2 Free body diagram of a strip element

$$\frac{\mathrm{d}s}{\mathrm{d}x} = -\frac{\mathrm{d}p}{\mathrm{d}x} \tag{22}$$

By Eqs. (21) and (22), the balance equation in the work zone can be simplified as

$$\sigma\frac{\mathrm{d}y}{\mathrm{d}x} - y\frac{\mathrm{d}p}{\mathrm{d}x} + 2\tau_{\mathrm{f}} = 0 \tag{23}$$

Friction stress τ_{f} is generated by the viscous shearing of lubrication oil film, so Eq. (23) can be expressed as

$$\tau_{\mathrm{f}} = \mu\frac{(u - v)}{h} \tag{24}$$

where μ is the lubricant viscosity. So the distribution of pressure stress and friction stress in the strip rolling process can be solved by numerical method from Eqs. (23) and (24). The interfacial coupling relationship diagram is schematically illustrated in Fig. 3.

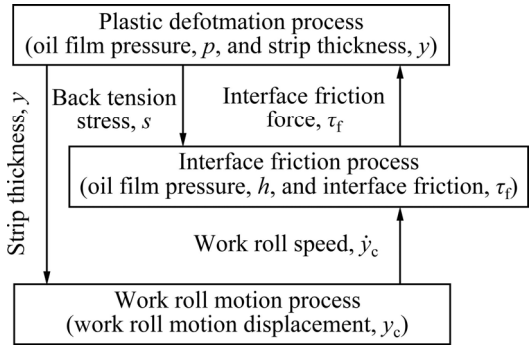

Fig. 3 Coupling relations of work interface

5 System dynamics analysis of rolling mill

Figure 4 shows a simplified vertical vibration model of the 1850 type rolling mill system. According to the characteristics of a 1850 type rolling mill in a large iron and steel plant, the system can be divided into six degrees of freedom vibration system with six qualities and seven springs. In the figure, m_1−m_6 represent the equivalent masses of the upper mill and the rack uprights of the rolling mill, the upper backup roll and its bearing and bearing seat, the upper work roll, the lower work roll, the lower backup roll and its bearing and bearing seat, and the rack lower beam, respectively. Stiffness k_1 is the equivalent stiffness of rack column and the upper beam; k_2 is the equivalent stiffness from the middle of the upper backup roll to the middle of the upper beam; k_3 is the elastic contact stiffness between the upper work roll and the upper backup roll; k_4 is the equivalent stiffness between the upper/lower work rolls and the strip under the rolling force P; k_5 is the elastic contact stiffness

between the lower work roll and the lower backup roll; k_6 is the equivalent stiffness from the middle of the lower backup roll to the middle of the lower beam; k_7 is the bending equivalent stiffness of the lower beam. In the model, the damping c_1 caused by the pressure cylinder above the upper backup roll, and the damping c_2 caused by the strip between the two work rolls are considered. Displacement $\{x\}$ is the vibration displacement increment of the various qualities. The simulation can be carried out by a computer program, which is compiled by using Microsoft Fortran Power Station Language.

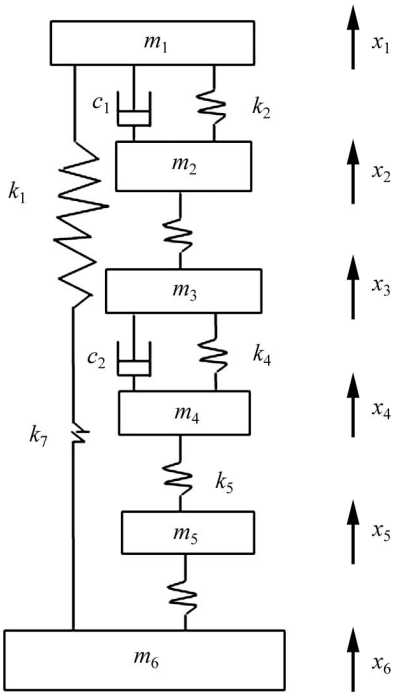

Fig. 4 Schematic illustration of 1850 type rolling mill vertical system model

The mathematical model of the rolling mill system with vertical vibration can be obtained as follows:

$$\boldsymbol{M}\{\ddot{x}\}+\boldsymbol{C}\{\dot{x}\}+\boldsymbol{K}\{x\}=\{P\} \tag{25}$$

where $\boldsymbol{M}$ is the mass matrix, $\boldsymbol{C}$ is damping matrix, $\boldsymbol{K}$ is stiffness matrix, and their specific expression are as follows:

$$\boldsymbol{M}=\begin{bmatrix} m_1 & 0 & 0 & 0 & 0 & 0 \\ 0 & m_2 & 0 & 0 & 0 & 0 \\ 0 & 0 & m_3 & 0 & 0 & 0 \\ 0 & 0 & 0 & m_4 & 0 & 0 \\ 0 & 0 & 0 & 0 & m_5 & 0 \\ 0 & 0 & 0 & 0 & 0 & m_6 \end{bmatrix}$$

$$\boldsymbol{C}=\begin{bmatrix} c_1 & -c_1 & 0 & 0 & 0 & 0 \\ -c_1 & c_1 & 0 & 0 & 0 & 0 \\ 0 & 0 & c_2 & -c_2 & 0 & 0 \\ 0 & 0 & -c_2 & c_2 & 0 & 0 \\ 0 & 0 & 0 & 0 & 0 & 0 \\ 0 & 0 & 0 & 0 & 0 & 0 \end{bmatrix}$$

$$\boldsymbol{K}=\begin{bmatrix} k_1+k_2 & -k_2 & 0 & 0 & 0 & 0 \\ -k_2 & k_2+k_3 & -k_3 & 0 & 0 & 0 \\ 0 & -k_3 & k_3+k_4 & -k_4 & 0 & 0 \\ 0 & 0 & -k_4 & k_4+k_5 & -k_5 & 0 \\ 0 & 0 & 0 & -k_5 & k_5+k_6 & -k_6 \\ 0 & 0 & 0 & 0 & -k_6 & k_6+k_7 \end{bmatrix}$$

6 Simulation results and discussion of oil film friction stress and pressure stress in roll gap

The rolling mill system parameters and the parameters of lubrication performance of a large company are listed in Table 1.

The simulated results of a large company 1850 rolling mill system are presented below. Numerical solving process can be carried out by a software Matlab. Figures 5 and 6 show the distribution situation of friction and pressure stress in the steady work zone. For smaller reduction (R=0.1 to 0.18), friction stress value is smaller, and the maximum friction stress is on the edge of the inlet and outlet (as shown in Fig. 5). This is because lubricant pressure stress under a smaller reduction is almost a constant. So lubrication viscosity is also a constant. The difference of surface speed of the roll and strip controls the distribution of the friction stress, and it is the biggest on the edge of the work zone. Under high reduction (R=0.2 to 0.25) case, the influence of the pressure and friction stress in the roll gap becomes very prominent and obvious.

Figures 7 and 8 show the distribution situation of pressure stress and friction stress in the unsteady work zone at different time. In the simulation analysis, assuming that back tension stress follows sin variation, back tension stress s respectively has the maximum 20 MPa, minimum 0 MPa and average 10 MPa at three different typical time. When the back tension stress (S= 20 MPa) is bigger, the pressure and friction stress in the work zone are smaller, the gradients of pressure and friction stress are also quite small, and the friction stress reaches maximum at the inlet and outlet edges, because

Table 1 Conditions for simulations and lubricant characteristics

y_1/mm	σ/MPa	S/MPa	R	a/mm	v_0/(m·s^{-1})	μ/(10^{-4}Pa·s)	Material
0.8	350	0−20	0.1−0.25	294	20	5.5	2A16

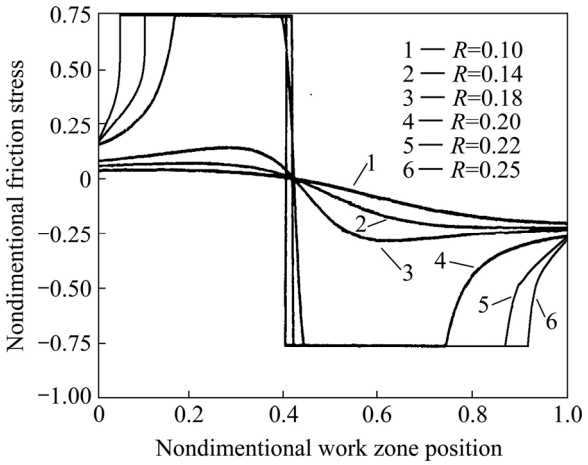

Fig. 5 Friction stress distributions for various reductions

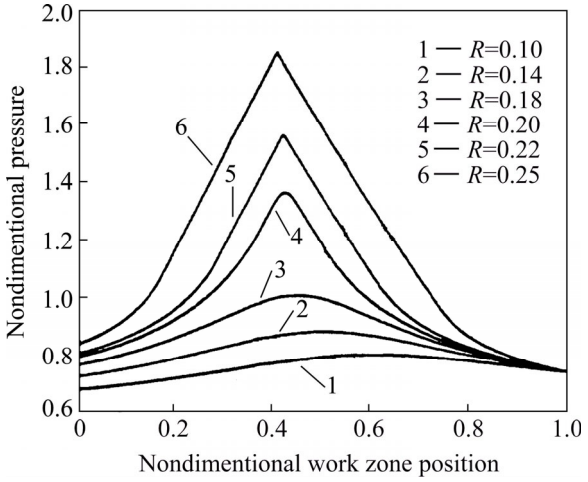

Fig. 6 Pressure distributions for various reductions

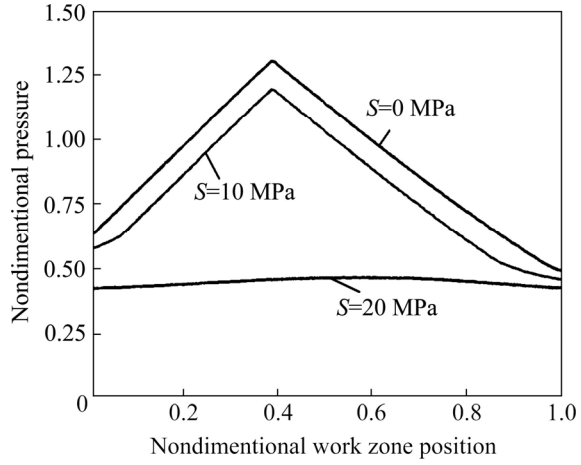

Fig. 7 Pressure distributions in work zone at different times

the relative sliding velocity of these two points are the largest. As the back tension stress decreases (S=10 MPa or 0 MPa), the pressure and the friction stress increase in the roll gap, and the pressure-sensitive lubricant viscosity increases exponentially with increasing pressure. So Figs. 7 and 8 demonstrate the unsteady (related to time) lubrication phenomenon in the roll bite.

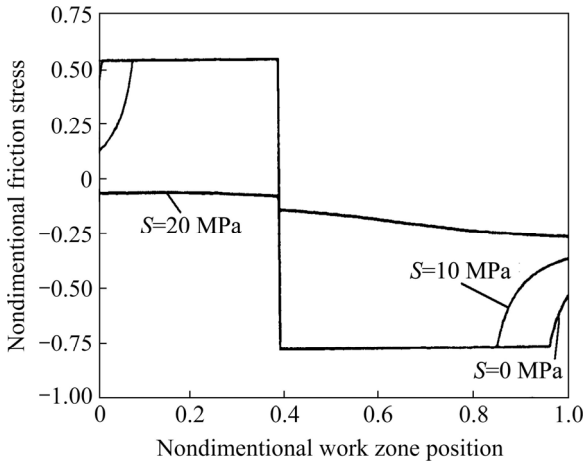

Fig. 8 Friction stress distributions in work zone at different times

7 Conclusions

1) A basic model is developed to analyze the unsteady lubrication film thickness, pressure and friction stress in the work zone in strip rolling.

2) When the back tension stress is bigger, the pressure and friction stress in the work zone are smaller, the gradients of pressure and friction stress are also quite small, and the friction stress reaches the maximum at the inlet and outlet edges.

3) As the back tension stress decreases, the pressure and the friction stress increase in the roll gap, and the pressure-sensitive lubricant viscosity increases exponentially with the increase of pressure.

References

[1] ZHENG Yong-jiang, XIE Zhao-hui, LI Yi-geng, SHEN Guang-xian, LIU Hong-min. Spatial vibration of rolling mills [J]. Journal of Materials Processing Technology, 2013, 213(4): 581−588.

[2] LI He-jie, JIANG Zheng-yi, WEI Dong-bin. Crystal plasticity finite modeling of 3D surface asperity flattening in uniaxial planar compression [J]. Tribology Letters, 2012, 46(2): 101−112.

[3] SUN Jian-liang, PENG Yan, LIU Hong-min. Non-linear vibration and stability of moving strip with time–dependent tension in rolling process [J]. Journal of Iron and Steel Research, International, 2010, 17(6): 11−15.

[4] YANG Xu, TONG Chao-nan, YUE Guang-feng, MENG Jian-ji. Coupling dynamic model of chatter for cold rolling [J]. Journal of Iron and Steel Research, International, 2010, 17(12): 30−34.

[5] XIANG Jun, HE Dan, ZENG Qing-yuan. Effect of cross-wind on spatial vibration responses of train and track system [J]. Journal of Central South University of Technology, 2009, 16(3): 520−524.

[6] SUN Cheng-gang. Investigation of interfacial behaviors between the strip and roll in hot strip rolling by finite element method [J]. Tribology International, 2005, 38(4): 413−422.

[7] ZHANG Bo, XU Bin-shi, XU Yi, ZHANG Bao-sen. Tribological characteristics and self-repairing effect of hydroxy-magnesium silicate on various surface roughness friction pairs [J]. Journal of Central South University of Technology, 2011, 18(5): 1326−1333.

[8] STEPHANY A, PONTHOT J P, COLLETTE C, SCHELINGS J. Efficient algorithmic approach for mixed-lubrication in cold rolling [J]. Journal of Materials Processing Technology, 2004, 153/154(11): 307−313.

[9] TIEU A K, JIANG Zheng-yi, LU Chen. A 3D finite element analysis of the hot rolling of strip with lubrication [J]. Journal of Materials Processing Technology, 2002, 125/126(9): 638−644.

[10] BENASCIUTTI D, BRUSA E, BAZZARO G. Finite elements prediction of thermal stresses in work roll of hot rolling mills [J]. Procedia Engineering, 2010, 2(1): 707−716.

[11] MOHAMMAD R F, IMAN S, AMIR H A. A comparative study of slab deformation under heavy width reduction by sizing press and vertical rolling using FE analysis [J]. Journal of Materials Processing Technology, 2009, 209(2): 728−736.

[12] KANG K, PELOW C, WITHAM L. Analysis of changes in 3D surface texture anisotropy ratio parameter and friction during sheet rolling campaigns [J]. Wear, 2008, 264(5/6): 434−438.

[13] GUO Rui, JIANG S H, CHOI Y H. Torsional vibration analysis of lathe spindle system with unbalanced workpiece [J]. Journal of Central South University of Technology, 2011, 18(1): 171−176.

[14] XIE Hai-bo, JIANG Zheng-yi, YUEN W Y D. Analysis of friction and surface roughness effects on edge crack evolution of thin strip during cold rolling [J]. Tribology International, 2011, 44(9): 971−979.

[15] TIEU A K, LIU Y J. Friction variation in the cold rolling process [J]. Tribology International, 2004, 37(2): 177−183.

[16] YUN I S, WILSON W R D, EHMANN K F. Review of chatter studies in cold rolling [J]. International Journal of Machine Tools and Manufacture, 1998, 38(12): 1499−1530.

[17] SANIEI M, SALIMI M. Development of a mixed film lubrication model in cold rolling [J]. Journal of Materials Processing Technology, 2006, 177(1/2/3): 575−581.

[18] WILSON W R D, CHANG D F. Low speed mixed lubrication of bulk metal forming processes [J]. ASME Journal of Tribology, 1996, 118(1): 83−89.

[19] ZHAO Zhi-ye. Metal plasticity deformation and roll theory [M]. Beijing: Metallurgical Industry Press, 1996: 96−98. (in Chinese)

(Edited by FANG Jing-hua)